An Adaptive Parameter Estimation in a BTV Regularized Image Super-Resolution Reconstruction

Mehdi MOFIDI[1], Hassan HAJGHASSEM[2], Ahmad AFIFI[1]
[1]*Department of Electrical Engineering, Malek Ashtar University of Technology, Tehran, Iran*
[2]*Department of New Sciences & Technologies, University of Tehran, Tehran, Iran*
m.mofidi@aletaha.ac.ir

***Abstract*—Access to the fine spatial resolution has always been a hotspot in digital imaging. One way to improve resolution is to use signal post-processing techniques. In this study, an improved multi-frame image super-resolution (SR) algorithm is proposed. The objective function should be minimized consists of a data error term, a regularization term and a regularization parameter. Based on the bilateral-total-variation (BTV) regularization, in the proposed method on one hand, the data error term incorporates frames with high accuracies in the reconstruction process, where an indicator weights each frame proportional to the frame error. On the other hand the regularization parameter is updated in each iteration based upon the Morozov's discrepancy principle. Iterative adjustment of the regularization parameter guarantees the SR solution to satisfy discrepancy principle. Visual evaluation and also quantitative measurements show that the performance of the proposed algorithm is better than of the several state-of-the-art methods.**

***Index Terms*—image processing, image reconstruction, maximum a posteriori, spatial resolution, statistical analysis.**

I. INTRODUCTION

The spatial resolution of an imaging system is always affected by hardware and physical constraints which lead to generate low-resolution (LR) images or sequence. However, in most applications high-resolution (HR) images are required and often desired. On the other hand, once an imaging system is manufactured, modifying the imaging hardware is not an available choice, thus highlighting a need for an image post-processing technique. One of these techniques is called super-resolution (SR) reconstruction which is a process that aims to fuse multiple LR images to compose a HR image. Generally, the relative sub-pixel motion between LR frames provides some redundant information which can be combined to produce a HR image. In SR literature, reconstruction-based algorithms are well developed in spatial domain. This can be due to their less sensitivity to errors and also more capability in incorporating prior knowledge about the HR image than the frequency domain [1]. The iterative back projection (IBP) [2], non-uniform interpolation [3], and the projection onto convex sets (POCS) [4] are such as non-statistical spatial domain approaches. Bayesian-based statistical algorithms, which are considered in this paper, consist of maximum likelihood (ML), maximum a posteriori (MAP), hybrid ML/MAP/POCS, variational Bayesian [5-9] and so forth. Since the SR reconstruction is an ill-posed problem, Bayesian regularized algorithms have become an appealing research topic in this area. This can be due to their strong statistical inference, robustness against the errors, and employment of priors as the regularization terms. A rich class of regularization-based functions is the MAP estimator. Generally, the MAP estimation can be formulated as the solution of a two-term optimization problem of the form [10]:

$$\min_{x_H}\left[C(x_H, x_L) + \lambda R(x_H)\right] \tag{1}$$

where $C(.)$ is the data error term, measuring lack of similarity to the data x_L, $R(.)$ is a measure of smoothness/roughness of solution which called regularization function and $\lambda > 0$ is the regularization parameter, attributing C and R. There are two key points in successfully solving the MAP-based super-resolution problem: 1) specification of the methods entail making choice of C and R, and 2) estimation of the regularization parameter λ that balance the relative weights between C and R. Estimators include Lorentzian, Huber, Tukeys' Biweight, L_1 and L_2 norms have been used as data error term C, in several works [10-13]. The L_1 norm has a good performance of preserving edges for the speckle noise model and misregistration errors, whereas the L_2 norm for Gaussian noise model can well keep the smoothness of the image. This motivates everyone to find a way which merges both advantages of L_2 and L_1 norms. The success of other above-mentioned estimators is highly dependent on accurate selection of their threshold values. As a choice of regularization term R, Tikhonov method [14] is one of the most classical regularization terms which introduces smoothness constraints in reconstructed image, but it loses sharpness in the HR image. Total variation (TV) [15] is another regularizer which overcomes the shortcoming of Tikhonov method and is widely used in image restoration tasks. A progressive regularization function presented in [16] based on a bilateral total variance (BTV) as a modification of TV method. We will also use BTV as regularization term, in our formulation.

As one of the objectives, we focus our attention on the second mentioned essential problem, finding the regularization parameter λ. However the wise choice of λ is a delicate object: if λ is too large, the super-resolved image is oversmoothed, and conversely, if λ is too small, the noise will not be effectively suppressed. In many works the regularization parameter is determined manually by trial-

Digital Object Identifier 10.4316/AECE.2017.03001

and-error. However, this procedure can be time-consuming and chanceful. To avoid these drawbacks, up to now, several adaptive selection strategies have been proposed. For example, the generalized cross-validation (GCV) method [17], the L-curve method [18], the U-curve method [19], the variational Bayesian framework [9], and the discrepancy principle [20]. The GCV method is based on *a-priori* knowledge of the input errors in LR frames [21] and it can be used when the regularization term is a quadratic function. It is well known that the computational cost of GCV is high [19]. The L-curve criterion is implemented by the plot of the norm of regularization term versus the norm of the corresponding data error term. Generally, the L-curve has a "vertical" part and a "horizontal" part. The optimum regularization parameter is located in the L-shaped corner of the L-curve. Sometimes, finding the exact corner of the curve is difficult. Moreover, to do so, one should solve (1) many times for different λ's. Another practical method is the U-curve criterion which has a similar procedure to L-curve method. The U-curve provides a truncated interval where the optimal λ locates. Therefore, as the main difference, U-curve has a reduced computational cost than the L-curve method. The variational Bayesian framework can provide good solutions, but since it is dependent on some attached parameters, it is not fully adaptive. In image restoration field with a single LR frame, based on the primal dual approach and discrepancy principle, an efficient TV-regularized restoration problem is handled in [22]. Another TV-based image restoration work using variable splitting technique is presented in [23] based on discrepancy principle. In this paper, in order to select the regularization parameter we use the Morozov's discrepancy principle, which less attention has given to it in super-resolution literature. This method chooses λ by adjusting the discrepancy between observed and expected images to some upper bounds. We should emphasize on major differences between our method and other methods using the discrepancy principle. Based upon our knowledge, most of the presented works are in image restoration field, not SR reconstruction, where only one LR frame is employed. These methods are based on TV regularization, suffer from their nondifferentiability. In this case some numerical methods including variable splitting algorithms [24] and primal dual model [22] should be employed which require to introduce some auxiliary variables [23]. Therefore, they are more complex than our algorithm, where BTV regularization is used and no variable is introduced in minimization problem. In addition, BTV method could preserve edges and suppress noise better than TV method [25]. Our objectives in this paper are twofold. First, we suggest a modified data error term which assigns proper weight to each frame based upon the frame error. In this strategy, frames with higher accuracies will have more contribution in SR reconstruction. Second, as a more adaptive solution, unlike the existing optimized methods that focus on problems with a fixed λ, we propose a discrepancy based regularization parameter selection in an adaptive way. The remainder of this paper is structured as follows: the observation model for image acquisition is provided in section II. Section III describes the proposed reconstruction model. Experimental results and discussion are given out in Section IV. Finally, a conclusion is drawn in Section V.

II. Imaging Observation Model

The degradation procedure in an imaging system can relate HR and LR frames through a mathematical forward model. Assuming the degradation involves downsampling, Gaussian blurring, warping and additive noise, the model can be expressed linearly as:

$$\underline{X}_L^k = DH_kF_k\underline{X}_H + E_k \tag{2}$$

where $\underline{X}_L^k$ denotes to the multiple LR images that are used to generate a single HR image($\underline{X}_H$) and k is the number of LR images ($k=1,2,\ldots,K$). In above forward model warping operator(F_k) encodes the motion information of the k –th LR frame to $\underline{X}_H$. Blurring effect is realized by applying the blurring kernel(H_k). The warped and blurred images are then downsampled by decimation operator D. $\underline{E}_k$ is the noise term that finally adds to the process. The matrices $\underline{X}_L^k$, D, H_k, F_k, $\underline{X}_H$ and $\underline{E}_k$ are of sizes $MN\times 1$, $MN\times r^2MN$, $r^2MN\times r^2MN$, $r^2MN\times r^2MN$, $r^2MN\times 1$ and $MN\times 1$, respectively, where r is the integer-valued interpolation factor.

III. Proposed Model for SR Reconstruction Based on Adaptive Terms

A. Data error term

Generally, in SR image reconstruction, a sequence of LR images is fused to produce a higher resolution image. In doing so, accurate motion estimation, precise mapping of the LR pixels on to the HR frame, and blurring kernel estimation/assumption is essential to the success of any SR algorithm. Moreover, noise model, noise level, and existence of outliers in the LR frames are as influential factors on the final result. Therefore, a robust estimation method that is not such sensitive to errors may produce more stable results. A pervasive family of estimators is the ML estimators. Based upon the ML concept, the estimation of $\hat{X}_H$ is done through the following minimization expression [13]:

$$\hat{X}_H = \arg\min_{X_H}\left[\sum_{k=1}^{K}\rho\left(DH_kF_k\underline{X}_H - \underline{X}_L^k\right)\right] \tag{3}$$

where $\rho(DH_kF_k\underline{X}_H - \underline{X}_L^k)$ is the data error term, measuring the "residual" between the observation and the estimation models. Defining x as the residual error, mathematically, $\rho(x)$ could be an even positive function with a unique minimizer at $x=0$ Derivative of $\rho(x)$ with respect to X_H, denoted $\varphi(x)=(\partial/\partial X_H)(\rho(x))$ is called the influence function, and can be used to define the bias that a particular observation has on the solution [26]. $\rho(x)$ should be chosen according to the distribution of the residual errors. Considering this, some proper choices for $\rho(x)$ are the L_1, L_2, and L_p norms ($0<p\le 1$). The error function of L_1 norm is $\rho(x)=|x|$, and $\varphi(x)=sign(x)$. Due to the constancy

and bounded value of influence function (-1 or 1), the L_1 norm doesn't distinguish between large errors corresponding by outliers or small errors caused by additive noise [27]. For L_2 norm, $\rho(x)=0.5x^2$ and therefore $\varphi(x)=x$ that obviously increases linearly and without bound with respect to x. This linear proportionality to residual errors causes the poor performance of L_2 norm in the presence of outliers or large errors [16]. As a result, L_1 norm is not sensitive to large errors but when the residual errors are relatively small, L_2 norm has a better performance than the L_1 norm. Moreover, L_1 does not have an analytical solution, but L_2 norm does. In such a situation, a model with a hybrid effect that has the advantages of both L_1 and L_2 norm terms can perform better than L_1 or L_2 norms. Various ML-estimators such as Lorentzian, Huber and Tukeys' Biweight are proposed in [11-13]. All of these estimators have a combinational behavior of both L_1 and L_2 norms which uses a threshold to define the behavior of error norm adaptively. In other words, for values smaller than a threshold the function follows L_2 norm and for values larger than threshold they perform like L_1 norm. Therefore, an adaptive threshold selection for these M-estimators has a key role in the success of super-resolution reconstruction. The Half-quadratic estimation is one of the adaptive error functions with above mentioned properties which is proposed in [27]:

$$\rho(x,a)=a\sqrt{a^2+x^2}-a^2 \tag{4}$$

where a is a positive number. $\rho(x,a)$ is convex and twice continuously differentiable which guarantees a unique solution of the optimization problem. The influence function of $\rho(x,a)$ is defined as:

$$\phi(x,a)=ax\Big/\sqrt{a^2+x^2} \tag{5}$$

with a fixed a, when x is relatively small, $\rho(x,a)\approx x^2/2$ and the function behaves like L_2 norm. On the other hand, when x is large enough, $\rho(x,a)\approx a|x|-a^2$ and the function takes the shape of L_1 norm. The selection of L_1 norm or L_2 norm and the transition between them can be controlled by modifying the parameter a. In other words, for large values of x (large errors), a should be small and conversely, for small values of x (small errors), a should be large. Accordingly, $\rho(x,a)$ is an adaptive robust norm. Substituting (4) in (3), after one step manipulation, one can result in:

$$\hat{X}_H=\arg\min_{X_H}\left[\sum_{k=1}^{K}a_k\sqrt{a_k^2+\left(DH_kF_k\underline{X}_H-\underline{X}_L^k\right)^2}-a_k^2\right] \tag{6}$$

where a_k is the threshold parameter for the k-th frame. Each of the LR frames can have its own a_k, due to the different accuracy of frames in registration step. In other words, a_k acts as a frame indicator which is inversely proportional to the frame errors. It is clear that, more erroneous frames should have less participation in the final HR result. A method for choosing a_k is proposed in [27], but it has a relative high computational cost. Herein, we introduce a new formulation for a_k, while simplicity, provides acceptable results. Considering $X_H(0)$ as the first HR estimation, a_k can be written as:

$$a_k=\sqrt{E_{k_{\max}}-E_{k_{\min}}}\Big/E_k^2 \tag{7}$$

where $E_k=\left\|DH_kF_k\underline{X}_H(0)-\underline{X}_L^k\right\|_2\Big/U$ is the k-th frame error term. $E_{k_{\max}}$ and $E_{k_{\min}}$ are the maximum and minimum of all E_k values, respectively. In this case, by increasing E_k, a_k will decrease and the frame weight in SR reconstruction will reduce. In our experiment, $X_H(0)$ is the up-scaled version of a random LR frame by bilinear interpolation.

B. Regularization using BTV function

Direct inversion of matrix multiplication DH_kF_k in (2), is not usually a viable approach due to its large dimensions and the ill-posedness of the problem [28]. In this case, regularization stabilizes the inverse problem appropriately, while providing a reasonable solution to the original problem. There are, however, different possibilities for the regularization term. One of the referenced functions called bilateral total variation (BTV) is proposed in [16] as a modification of TV method:

$$R_{BTV}(X_H)=\sum_{l=-P}^{P}\sum_{m=-P}^{P}\alpha^{|m|+|l|}\left\|\underline{X}_H-S_x^lS_y^m\underline{X}_H\right\|_1 \tag{8}$$

where S_x^l and S_y^m shift X_H by l and m pixels in the x and y directions, respectively. The weight $0<\alpha<1$ imposes a spatial decaying effect to regularization terms and P defines the size of the regularization kernel. BTV method is computationally efficient, and it tends to preserve edges. By substituting data error term (6) and regularization term (8) in (1), the desired solution X_H can be obtained efficiently using iterative methods like steepest descent (SD) algorithm through $X_H^{i+1}=X_H^i-\beta\nabla X_H^i$. In this equation, i refer to the iteration number, β is the step size in the negative direction of the gradient and ∇ is the derivative operator. Accordingly, optimal X_H can be found, as follows:

$$\begin{aligned}X_H^{i+1}=X_H^i-\beta\Bigg(&\sum_{k=1}^{K}\left(DH_kF_k\right)^TA_k\left(DH_kF_k\underline{X}_H^i-\underline{X}_L^k\right)\\&+\lambda\sum_{l=-P}^{P}\sum_{m=-P}^{P}\alpha^{|l|+|m|}\left[I-S_x^{-l}S_y^{-m}\right]sign\left(\underline{X}_H^i-S_x^lS_y^m\underline{X}_H^i\right)\Bigg)\end{aligned} \tag{9}$$

where S_x^{-l} and S_y^{-m} are the transpose of S_y^l and S_y^m, respectively and $A_k=a_k\Big/\sqrt{a_k^2+\left(DH_kF_k\underline{X}_H^i-\underline{X}_L^k\right)^2}$. Regularization parameter λ has a vital role in the optimization process. In the following, we propose a strategy to choose regularization parameter adaptively, in each iteration of optimization.

C. Adaptive method for regularization parameter selection

One of the main operational problems in (1) (as well as in (9)) is how to choose the regularization parameter λ. There are different posteriori strategies for choosing λ in the literature. In this regard, we will use the Morozov's

discrepancy principle which has been studied less in SR reconstruction. One can assume that the discrepancy between the observed and the estimated frames is defined as:

$$e^{i+1}(\lambda)=\sum_{k=1}^{K}\left(X_L^k-DH_kF_kX_H^{i+1}\right) \tag{10}$$

According to this principle, a good solution of the image restoration problem based on a single frame should lie in $\|X_L-DHFX_H\|_2^2\le mn\sigma^2$ [29], where σ^2 is the variance of the noise. In the case of image super-resolution problem, where K is the number of LR frames, we can express:

$$\left\|e^{i+1}(\lambda)\right\|_2^2\le Kmn\sigma^2 \tag{11}$$

where $\left\|e^{i+1}(\lambda)\right\|_2^2$ is a positive and decreasing convex function of λ. It means that if the noise power is known, (11) provides a bound on discrepancy $e^{i+1}(\lambda)$. So in particular, parameter λ^{i+1} in the $(i+1)$-th iteration could be chosen by requiring $\left\|e^{i+1}(\lambda)\right\|_2^2=Kmn\sigma^2$ By substituting X_H^{i+1} from (9) in (10) the following formula can be written:

$$e^{i+1}(\lambda)=\sum_{k=1}^{K}\left(X_L^k-DH_kF_k\left(X_H^i-\beta\left(G_1+\lambda G_2\right)\right)\right) \tag{12}$$

where G_1 and G_2 are the derivatives of data error term and regularization term, respectively:

$$G_1=\left(\sum_{k=1}^{K}\left(DH_kF_k\right)^T\left(a_k\Big/\sqrt{a_k^2+\left(DH_kF_k\underline{X}_H^i-\underline{X}_L^k\right)^2}\right)\left(DH_kF_k\underline{X}_H^i-\underline{X}_L^k\right)\right) \tag{13}$$

$$G_2=\left(\sum_{l=-P}^{P}\sum_{m=-P}^{P}\left(\alpha^{|l|+|m|}\left[I-S_x^{-l}S_y^{-m}\right]sign\left(\underline{X}_H^i-S_x^lS_y^m\underline{X}_H^i\right)\right)\right) \tag{14}$$

By separating the terms involving parameter λ from the others in (12), we will have:

$$e^{i+1}(\lambda)=A+\lambda B \tag{15}$$

where:

$$A=\sum_{k=1}^{K}\left(X_L^k-DH_kF_k\left(X_H^i-\beta G_1\right)\right) \tag{16}$$

$$B=\sum_{k=1}^{K}\left(DH_kF_k\beta G_2\right) \tag{17}$$

Since $\left\|e^{i+1}(\lambda)\right\|_2^2=\left(e^{i+1}(\lambda)\right)^T\left(e^{i+1}(\lambda)\right)$, by substituting (15) in this equation, after some manipulation, one can express:

$$\left\|e^{i+1}(\lambda)\right\|_2^2=A^TA+\lambda(A^TB+B^TA)+\lambda^2B^TB \tag{18}$$

Finally by equating (18) to $Kmn\sigma^2$, λ can be calculated in each iteration. As can be seen, this calculation requires solving a nonlinear equation in order to obtain the value of the regularization parameter λ. We use the Gauss-Newton algorithm to find λ iteratively. The resulting algorithm for SR reconstruction is summarized in Fig.1.

IV. Experimental Results

To evaluate the performance of the proposed SR algorithm, simulation experiments are carried out in MATLAB R2009a environment on a laptop computer with Intel core i5 processor running at 2.53 GHz clock with an 8GB internal RAM memory.

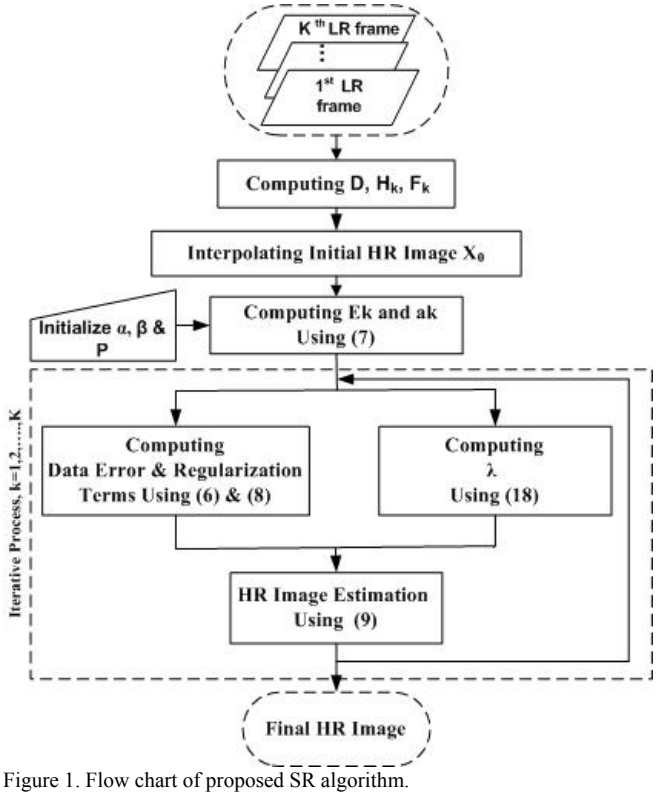

Figure 1. Flow chart of proposed SR algorithm.

The experiments consist of two parts. In the first part (Subsection A), the experiments come to test the performance of proposed algorithm on some synthetic images.

The LR images in this part are acquired from a single-frame HR image by a degradation procedure which is described in the same section. In the second part (Subsection B), we turn to real images in order to test the effectiveness of the SR model. In both subsections, the performance of data error term is investigated first. To this end, at first, regularization term (BTV) is kept constant and λ is selected manually to have a fair comparison with other two methods. By fixing the regularization term, we justify the effectiveness of our proposed data error term, by comparing it with the L_1 norm [16] "denoted as L_1+BTV" and L_2 norm [30] "denoted as L_2+BTV". Furthermore, the results of proposed method with manual selection of regularization parameter and Half-quadratic method [30] are presented. In the next experiment, adaptive selection of λ using the proposed method is compared with GCV [17] and L-Curve [18] methods which are applied for automatic selection of regularizing parameter.

A. Synthetical experiments

In this section, two original *Remote Sensing* images of sizes 360×360 pixels are chosen which are depicted in Fig. 2(b) and Fig. 3(b). Four LR *Remote Sensing* images are generated by shifting Fig. 2(b) and Fig. 3(b) horizontally and vertically, blurring them with a zero-mean 5×5 Gaussian kernel with standard deviation of 1, and downsampling them by factor of 2. Figs. 2(a) and 3(a) show one of the resulted LR frames (of size 180×180) in each *Remote sensing* images. It should be noted that the SR model parameters such as motion vectors (F_k), blurring kernels (H_k), and additive noise (E_k) are unknown and

needed to be estimated. In the experiments, an efficient phased based image matching method [31] is employed for motion estimation. After this step, H_k is assumed to be a 5×5 Gaussian kernel with standard deviation equal to 1. We used the method described in [32] to estimate the additive noise variance. The values of fixed parameters in SR model are as follows: $\alpha = 0.5$ and $P = 2$. For a fair evaluation of performance, the parameters of other existing algorithms are chosen in several trials to produce most appealing results. To facilitate a better comparison, a region is cropped and shown at the bottom-right of each image. Fig. 2(c) and Fig. 3(c) show the result of using L_2+BTV algorithm. From this result, it is clear that L_2 norm suffers from obvious noise and artifacts. Observation from Fig. 2(d) and Fig. 3(d) suggest that the use of L_1+BTV term, in spite of suppressing the noise and artifacts, reduces the image quality significantly. This might be because L_2 norm differentiates between large errors and small errors, and assigns a distinct weight to each one. Whereas L_1 assigns identical weights to all errors and this mode creates it more undesirable compared to L_2 norm. As shown in Fig. 2(e) and Fig. 3(e), unlike L_2+BTV and L_1+BTV cases, the Half-quadratic method proposed in [27] has a better visual results but it lacks sharp edges and fine details.

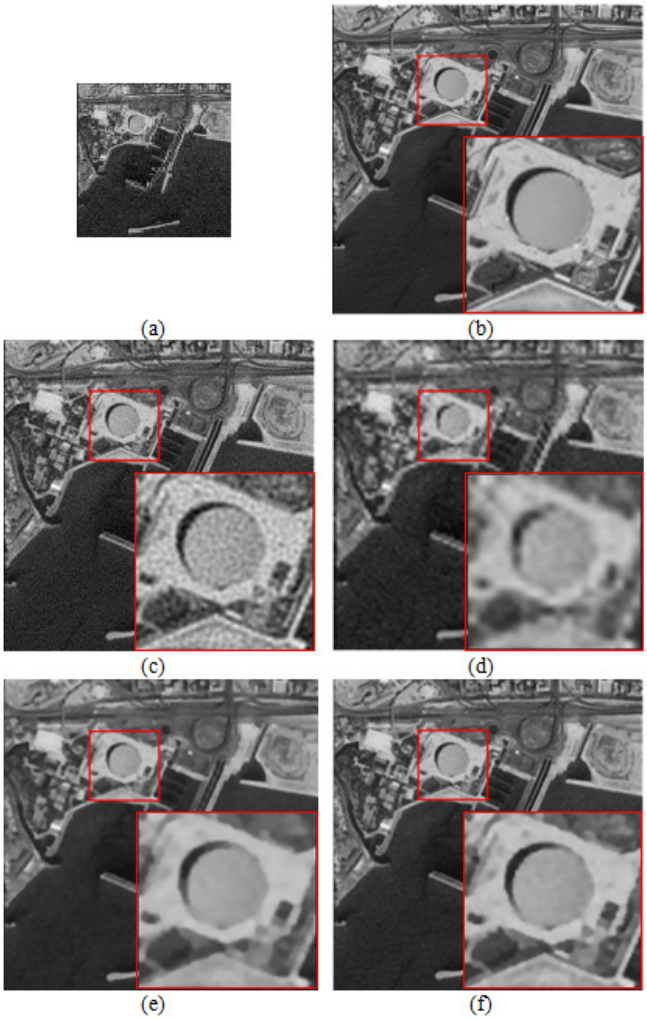

Figure 2. Reconstruction results of *Remote Sensing1* sequence. (a) One of LR-Images, (b) original HR-Image, (c) result of L_2+BTV, (d) result of L_1+BTV, (e) result of Half-quadratic method, and (f) result of proposed method with manual selection of λ.

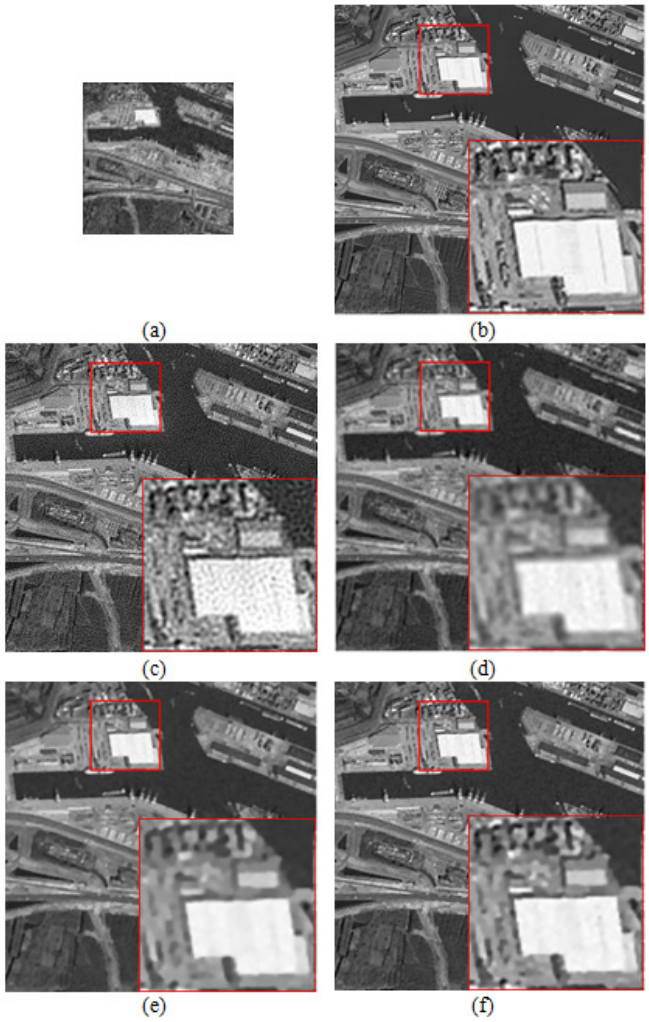

Figure 3. Reconstruction results of Remote Sensing2 sequence. (a) One of LR-Images, (b) original HR-Image, (c) result of L2+BTV, (d) result of L1+BTV, (e)result of Half-quadratic method, and (f) result of proposed method with manual selection of λ.

Fig. 2(f) and Fig. 3(f) show the reconstruction result of proposed method under the manual selection of regularization term. This may, in part, be caused by adaptive data error term which assigns smaller weights a_k to the LR frames that are corrupted by more errors.

In this subsection, we have judged the quality of reconstructed image quantitatively by well-known peak signal-to-noise ratio (PSNR) and structural similarity (SSIM) [33-34] indices. It should be mentioned that in this part, regularization parameter is selected manually for better comparison of data error terms.

TABLE I. PSNR AND SSIM VALUES FOR FIGURE 2 AND FIGURE 3

Image	Method	PSNR(dB)	SSIM
Remote Sensing1	L_2+BTV	26.1952	0.5478
	L_1+BTV	21.6908	0.577
	GCV	22.4791	0.6115
	L-curve	24.4821	0.6881
	Half_quadratic	25.3732	0.7146
	Proposed_manual	26.5292	0.7304
	Proposed_adaptive	**26.9464**	**0.7671**
Remote Sensing2	L_2+BTV	23.0101	0.6008
	L_1+BTV	21.3949	0.6150
	GCV	21.5683	0.6002
	L-curve	21.6696	0.6227
	Half_quadratic	22.2084	0.6463
	Proposed_manual	23.1147	0.6811
	Proposed_adaptive	**23.4606**	**0.7047**

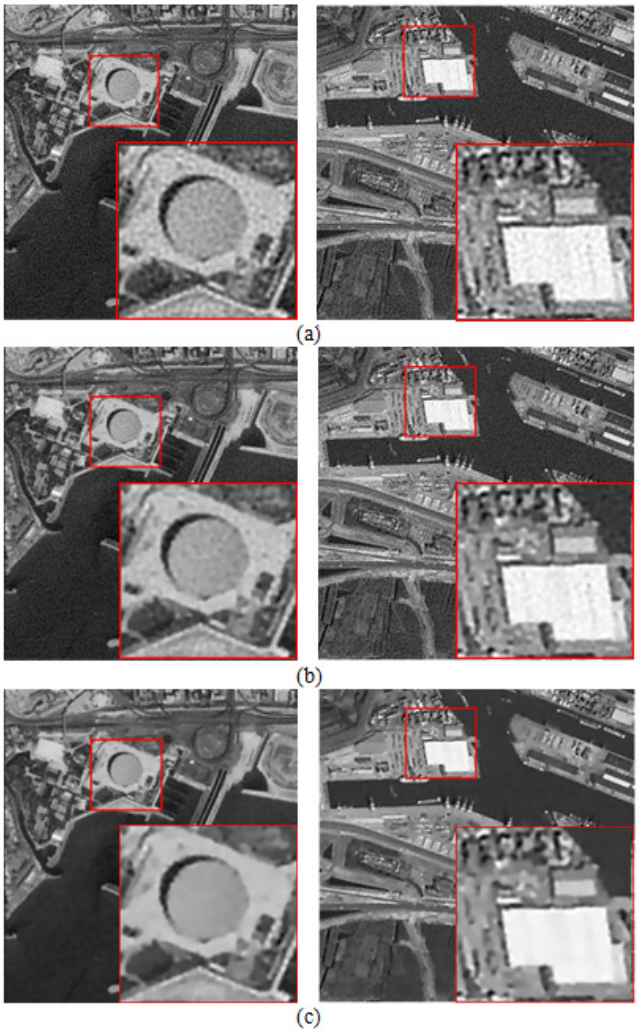

Figure 4. Reconstruction results of *Remote Sensing1* and *Remote Sensing2* sequences. (a) result of GCV, (b) result of L-curve, and (c) result of proposed method with adaptive selection of λ.

However, the results of the proposed method by automatically selecting λ are also reported in Table I. Evidently, from Table I, we can see that our proposed method outperforms other methods and achieves the highest PSNR and SSIM results.

Fig. 4 compares GCV and L-curve algorithms with proposed method, which all of them are used for automatic selection of λ. As can be seen, GCV method adds a considerable noise to the resulted image. Noise of L-curve is less than the noise added by GCV but still quality of the image is poor. Finally, based on proposed method in Fig. 4, noise is eliminated considerably, however edges are sharper.

For better quantitative comparison of data error terms, the effect of varying regularization parameter λ on SSIM values is plotted for different methods in *Remote sensing1* and *Remote sensing2* images. As can be seen in Figs. 5(a) and 5(b), the proposed method has allocated a higher numerical result (SSIM) for all values of λ. Half-quadratic method also shows an appropriate behavior, but it ranks second in terms of performance. In general, L_1+BTV and L_2+BTV methods are ranked 3rd and 4th, respectively.

Fig. 6 shows performance of the mentioned methods for automatic selection of λ based on number of iterations and SSIM value. Less iterations for achieving a higher SSIM in proposed method is a key point which indicates simplicity and better performance of this algorithm.

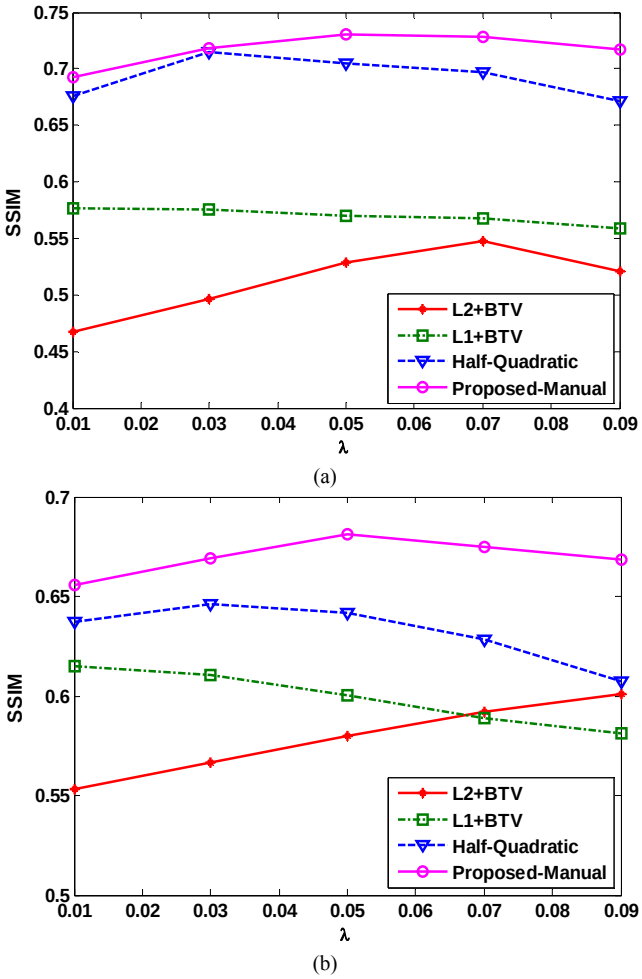

Figure 5. SSIM versus regularization parameter λ, (a) result for Remote Sensing1, (b) result for Remote Sensing2.

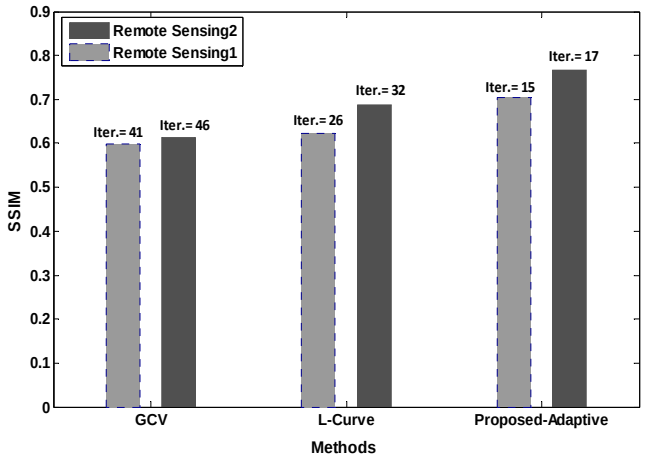

Figure 6. Performance of different regularization parameter selection methods in terms of iteration number and SSIM value.

For example, it can be seen that for obtaining an identical SSIM, the number of iterations in proposed method is 1/3 of GCV method.

B. Real-world experiments

For a better comparison, proposed method is also applied to the real sequence "*text*". This sequence consists of 30 images (of size 57×49 pixels). Considering zoom factor of 4, after SR reconstruction resolution of images reach to 228×196 pixels. The motion vectors (F_k), blurring kernels (H_k), and additive noise (E_k) in SR model are unknown

which are estimated in the same way of the previous section.

In the real-world experiment, since no ground truth HR image is available, the reconstruction results can be assessed by a no-reference image quality measure. Metric-Q and cumulative probability of blur detection (CPBD) are two image quality measures proposed in [35] and [36], respectively. Metric-Q employs the singular value decomposition of the local image gradients to evaluate the sharpness and contrast of reconstructed image. According to the Metric-Q, the higher the value is, the better the sharpness and the contrast will be. CPBD measure mainly assesses the image sharpness. CPBD ranges in [0-1] and the higher the value is, the better the sharpness will be.

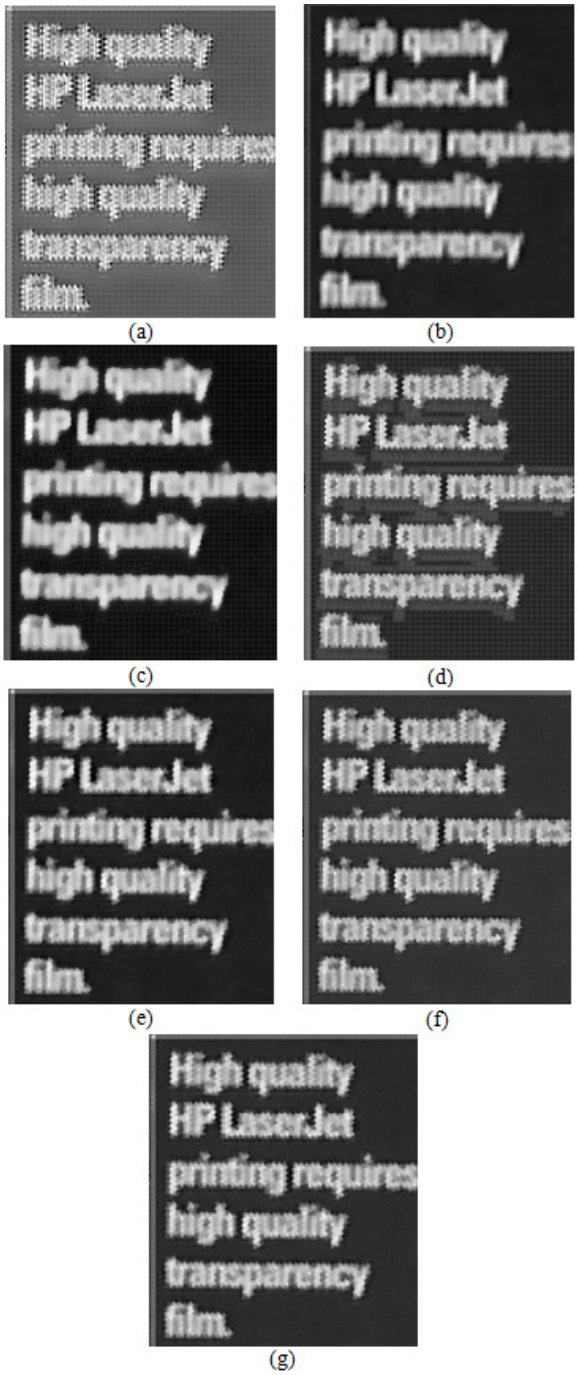

Figure 7. Reconstruction results of real sequence *text*. (a) result of L_2+BTV, (b) result of L_1+BTV, (c) result of Half-quadratic method, (d) result of GCV, (e) result of L-curve, (f) result of proposed method with manual selection of λ, and (g) result of proposed method with adaptive selection of λ.

TABLE II. CPBD AND METRIC_Q VALUES FOR FIGURE 7

Image	Method	CPBD	Metric_Q
	L_2+BTV	0.4517	18.5375
	L_1+BTV	0.4351	19.5519
	GCV	0.4493	19.0984
text	L-curve	0.4548	19.8322
	Half_quadratic	0.4273	19.6978
	Proposed_manual	0.4554	19.9216
	Proposed_adaptive	**0.4695**	**20.0893**

As can be seen in Fig. 7 (a), result of L_2+BTV norm is an output with boosted effect of noise which can be due to its non-robust behavior against large errors. Although in Fig. 7(b), L_1+BTV has a successful noise removal, but the image is oversmoothed and the details are destroyed. Result obtained from Half-quadratic method Fig. 7 (c) is still blurred. Due to Fig. 7 (d), applying GCV method for automatic selection of λ creates considerable artifacts and noise. Fig. 7 (e) is obtained from L-curve which gives better results than GCV method.

Finally, In Figs. 7 (f) and (g) which are obtained from proposed method with manual and automatic λ, respectively, identifying characters in images is better than other methods. The Metric-Q and CPBD values for each approach are reported in Table II which validate our proposed method gives the highest quantitative measurement values. However, one can compare these methods in terms of time constraints in real-time applications.

V. CONCLUSION

In this study, an adaptive algorithm is proposed to address data error term selection and regularization parameter estimation in an image SR reconstruction. At first, in the data error counterpart, we have employed a simple but efficient weighting factor which incorporates less erroneous LR frames in the SR reconstruction. Then, based on BTV regularization, we have formulated the problem as finding the regularization parameter which satisfies the Morozov's discrepancy principle. Selecting the frames with lower error in data error term, efficient method for choosing the λ (direct solving without using auxiliary variables), higher algorithm speed in λ selection (fewer number of iterations than other automatic selection methods of λ) are among the achievements of this study. We have applied several experiments on some synthesized and real LR frames. Both visual and quantitative evaluation results show that the proposed algorithm can provide more appealing results than the other compared methods.

REFERENCES

[1] S. C. Park, M. K. Park, M. G. Kang, "Super-resolution image reconstruction: a technical overview," IEEE Signal Process. Mag., vol. 20, no. 3, pp. 21–36, May 2003. doi:10.1109/MSP.2003.1203207

[2] M. N. Bareja, C. K. Modi, "An improved iterative back projection based single image super resolution approach," Int. J. Image Graph., vol. 14, no. 04, p. 1450015, Oct. 2014. doi:10.1142/S0219467814500156

[3] T. Lukes, K. Fliegel, M. Klima, "Objective image quality assessment of multiframe super-resolution methods," in Proc. 23rd International Conference Radioelektronika, Czech Republic, 2013, pp. 267–272. doi:10.1109/RadioElek.2013.6530929

[4] T. Wang, L. Cao, W. Yang, Q. Feng, W. Chen, Y. Zhang, "Adaptive patch-based POCS approach for super resolution reconstruction of 4D-CT lung data," Phys. Med. Biol., vol. 60, no. 15, pp. 5939–5954, Aug. 2015. doi:10.1088/0031-9155/60/15/5939

[5] P. Vandewalle, L. Sbaiz, J. Vandewalle, M. Vetterli, "Super-resolution from unregistered and totally aliased signals using subspace methods," IEEE Trans. Signal Process., vol. 55, no. 7, pp. 3687–3703, Jul. 2007. doi:10.1109/TSP.2007.894257

[6] M. K. Ng, A. C. Yau, "Super-resolution image restoration from blurred low-resolution images," J. Math. Imaging Vis., vol. 23, no. 3, pp. 367–378, Nov. 2005. doi:10.1007/s10851-005-2028-5

[7] M. Shen, C. Wang, P. Xue, W. Lin, "Performance of reconstruction-based super-resolution with regularization," J. Vis. Commun. Image Represent., vol. 21, no. 7, pp. 640–650, 2010. doi:10.1016/j.jvcir.2010.04.003

[8] L. T. Shao, H. G. Zhang, G. H. Zhang, "The improved hybrid MAP-POCS based algorithm for super-resolution image restoration research," Appl. Mech. Mater., vol. 701–702, pp. 373–380, Dec. 2014. doi:10.4028/www.scientific.net/AMM.701-702.373

[9] S. D. Babacan, R. Molina, A. K. Katsaggelos, "Parameter estimation in TV image restoration using variational distribution approximation," IEEE Trans. Image Process., vol. 17, no. 3, pp. 326–339, Mar. 2008. doi:10.1109/TIP.2010.2080278

[10] P. Milanfar, "Super-Resolution Imaging", pp. 9-23,CRC Press, 2011.

[11] V. Patanavijit, S. Jitapunkul, "A robust iterative multiframe super-resolution reconstruction using a Huber bayesian approach with Huber-Tikhonov regularization," in Proc. 2006 International Symposium on Intelligent Signal Processing and Communications, Yonago, Japan, 2006, pp. 13–16. doi:10.1109/ISPACS.2006.364825

[12] V. Patanavijit, S. Jitapunkul, "A robust iterative multiframe super-resolution reconstruction using a bayesian approach with Tukey's biweight," in Proc. 2006 8th international Conference on Signal Processing, Beijing, China, 2006. doi:10.1109/ICOSP.2006.345547

[13] V. Patanavijit, S. Jitapunkul, "A lorentzian stochastic estimation for a robust iterative multiframe super-resolution reconstruction with Lorentzian-Tikhonov regularization," EURASIP J. Adv. Signal Process., vol. 2007, no. 1, p. 034821, 2007. doi:10.1155/2007/34821

[14] A. A. Hefnawy, "An efficient super-resolution approach for obtaining isotropic 3-D imaging using 2-D multi-slice MRI," Egypt. Informatics J., vol. 14, no. 2, pp. 117–123, 2013. doi:10.1016/j.eij.2013.03.003

[15] Q. Yuan, L. Zhang, H. Shen, "Regional spatially adaptive total variation super-resolution with spatial information filtering and clustering," IEEE Trans. Image Process., vol. 22, no. 6, pp. 2327–2342, Jun. 2013. doi:10.1109/TIP.2013.2251648

[16] S. Farsiu, M. D. Robinson, M. Elad, P. Milanfar, "Fast and robust multiframe super resolution," IEEE Trans. Image Process., vol. 13, no. 10, pp. 1327–1344, Oct. 2004. doi:10.1109/TIP.2004.834669

[17] V. Moram, S. D. Cabrera, "Superresolution using the optimal recovery framework with automatic generalized cross-validation," in Proc. Digital Signal Processing and Signal Processing Education Meeting (DSP/SPE), USA, 2011, pp. 344–349. doi:10.1109/DSP-SPE.2011.5739237

[18] H. Z. Wang, S. Zhao, H.W. Lv, "Super-resolution image restoration with L-Curve," in Proc. 2008 Congress on Image and Signal Processing, China, 2008, pp. 597–601. doi:10.1109/CISP.2008.444

[19] Q. Yuan, L. Zhang, H. Shen, P. Li, "Adaptive multiple-frame image super-resolution based on U-curve," IEEE Trans. Image Process., vol. 19, no. 12, pp. 3157–3170, Dec. 2010. doi:10.1109/TIP.2010.2055571

[20] V. A. Morozov, "Methods for Solving Incorrectly Posed Problems", pp. 32-153, Springer Press, New York, 1984. doi:10.1007/978-1-4612-5280-1

[21] D. Krawczyk-Stańdo, M. Rudnicki, "Regularization parameter selection in discrete ill-posed problems - the use of the U-Curve," Int. J. Appl. Math. Comput. Sci., vol. 17, no. 2, pp. 157–164, Jan. 2007. doi:10.2478/v10006-007-0014-3

[22] Y. W. Wen, R. H. Chan, "Parameter selection for total-variation-based image restoration using discrepancy principle," IEEE Trans. Image Process., vol. 21, no. 4, pp. 1770–1781, Apr. 2012. doi:10.1109/TIP.2011.2181401

[23] C. He, C. Hu, W. Zhang, B. Shi, "A fast adaptive parameter estimation for total variation image restoration," IEEE Trans. Image Process., vol. 23, no. 12, pp. 4954–4967, Dec. 2014. doi:10.1109/TIP.2014.2360133

[24] M. V Afonso, J. M. Bioucas-Dias, M. A. T. Figueiredo, "An augmented lagrangian approach to the constrained optimization formulation of imaging inverse problems," IEEE Trans. Image Process., vol. 20, no. 3, pp. 681–695, Mar. 2011. doi:10.1109/TIP.2010.2076294

[25] P. Purkait, B. Chanda, "Super resolution image reconstruction through bregman iteration using morphologic regularization," IEEE Trans. Image Process., vol. 21, no. 9, pp. 4029–4039, Sep. 2012. doi:10.1109/TIP.2012.2201492

[26] A. Panagiotopoulou, V. Anastassopoulos, "Regularized super-resolution image reconstruction employing robust error norms," Opt. Eng., vol. 48, no. 11, p. 117004, Nov. 2009. doi:10.1117/1.3265543

[27] X. Zeng, L. Yang, "A robust multiframe super-resolution algorithm based on half-quadratic estimation with modified BTV regularization," Digit. Signal Process., vol. 23, no. 1, pp. 98–109, Jan. 2013. doi:10.1016/j.dsp.2012.06.013

[28] H. Song, L. Qing, Y. Wu, X. He, "Adaptive regularization-based space–time super-resolution reconstruction," Signal Process. Image Commun., vol. 28, no. 7, pp. 763–778, Aug. 2013. doi:10.1016/j.image.2013.03.008

[29] J. F. Aujol, G. Gilboa, "Constrained and SNR-based solutions for TV-Hilbert space image denoising," J. Math. Imaging Vis., vol. 26, no. 1–2, pp. 217–237, Nov. 2006. doi:10.1007/s10851-006-7801-6

[30] A. Panagiotopoulou, V. Anastassopoulos, "Super-resolution image reconstruction techniques: trade-offs between the data-fidelity and regularization terms," Inf. Fusion, vol. 13, no. 3, pp. 185–195, Jul. 2012. doi:10.1016/j.inffus.2010.11.005

[31] B. Setiyono, M. Hariadi, M. H. Purnomo, "Survey of super-resolution using phased based image matching," Journal of Theoretical and Applied Information Technology, Vol. 43, pp. 245-253, Sep. 2012.

[32] J. Immerkær, "Fast noise variance estimation," Comput. Vis. Image Underst., vol. 64, no. 2, pp. 300–302, Sep. 1996. doi:10.1006/cviu.1996.0060

[33] Z. Zheng Liu, R. Laganiere, "On the use of phase congruency to evaluate image similarity," in Proc. 2006 IEEE International Conference on Acoustics Speech and Signal Processing Proceedings, France, 2006, pp. II–937–II–940. doi:10.1109/ICASSP.2006.1660498

[34] Z. Wang, A. C. Bovik, H. R. Sheikh, E. P. Simoncelli, "Image quality assessment: from error visibility to structural similarity," IEEE Trans. Image Process., vol. 13, no. 4, pp. 600–612, Apr. 2004. doi:10.1109/TIP.2003.819861

[35] X. Zhu, P. Milanfar, "Automatic parameter selection for denoising algorithms using a no-reference measure of image content," IEEE Trans. Image Process., vol. 19, no. 12, pp. 3116–32, Dec. 2010. doi:10.1109/TIP.2010.2052820

[36] N. D. Narvekar, L. J. Karam, "A no-reference image blur metric based on the cumulative probability of blur detection (CPBD)," IEEE Trans. Image Process., vol. 20, no. 9, pp. 2678–2683, Sep. 2011. doi:10.1109/TIP.2011.2131660